Sedimentology (1996) **43**, 41–52

Field measurements of the flux and speed of wind-blown sand

RONALD GREELEY, DAN G. BLUMBERG and STEVEN H. WILLIAMS*
Department of Geology, Arizona State University, Box 871404, Tempe, AZ 85287–1404, USA

ABSTRACT

A field experiment was conducted to measure the flux and speed of wind-blown sand under known conditions in a natural setting. The experiment, run at Pismo Beach, California, involved a tract 100 m long (parallel with the wind) by 20 m wide. The site was instrumented with four arrays of anemometers to obtain wind velocity profiles through the lower atmospheric boundary-layer, temperature probes to determine atmospheric stability and wind vanes to determine wind direction. From these measurements, wind friction speeds were derived for each experimental run. In order to measure sand saltation flux, a trench 3 m long by 10 m wide (transverse to the wind direction) by 0·5 m deep was placed at the downwind end of the tract and lined with 168 collector bins, forming an 'egg-box' pattern. The mass of particles collected in each bin was determined for four experimental runs. In order to assess various sand-trap systems used in previous experiments, 12 Leatherman traps, one Fryberger trap and one array of Ames traps were deployed to collect particles concurrently with the trench collection. Particle velocities were determined from analysis of high-speed (3000 and 5000 frames per second) motion pictures and from a particle velocimeter. Sand samples were collected from the trench bins and the various sand traps and grain size distributions were determined. Fluxes for each run were calculated using various previously published expressions, and then compared with the flux derived from the trench collection. Results show that Bagnold's (1941) model and White's (1979) equation most closely agree with values derived from the trench. Comparison of the various collector systems shows that the Leatherman and Ames traps most closely agree with the flux derived from the trench, although these systems tended to under-collect particles. Particle speeds were measured from analysis of motion pictures for saltating particles in ascending and descending parts of their trajectories. Results show that particle velocities from the velocimeter are in the range 0·5–7·0 m s^{-1}, compared to a wind friction velocity of 0·32–0·43 m s^{-1} and a wind velocity of 2·7–3·9 m s^{-1} at the height of the particle measurements. Descending particles tended to exceed the speeds of ascending particles by $\sim$0·5 m s^{-1}.

INTRODUCTION

Wind has the potential for transporting large amounts of sand (i.e. particles 60–2000 μm in diameter). Several approaches have been used to study the flux of wind-blown sand, including field measurements (e.g. Owens, 1927; Belly, 1964; Leatherman, 1978; Fryberger *et al.*, 1984; Sarre, 1987), use of wind tunnels under controlled conditions (e.g. Bagnold, 1941; Rasmussen & Mikkelsen, 1991) and analytical approaches (e.g. Anderson & Hallet, 1986; Sorensen, 1991). The speeds of saltating particles have been measured in wind tunnels (e.g. White & Schulz, 1977; Greeley *et al.*, 1982; Willetts & Rice, 1986),

*Present address: Department of Space Studies, Center for Aerospace Sciences, University of North Dakota. Correspondence: Ronald Greeley, Department of Geology, Arizona State University, Tempe, AZ 85287–1404, USA. E-mail (Internet): Greeley@asu.edu

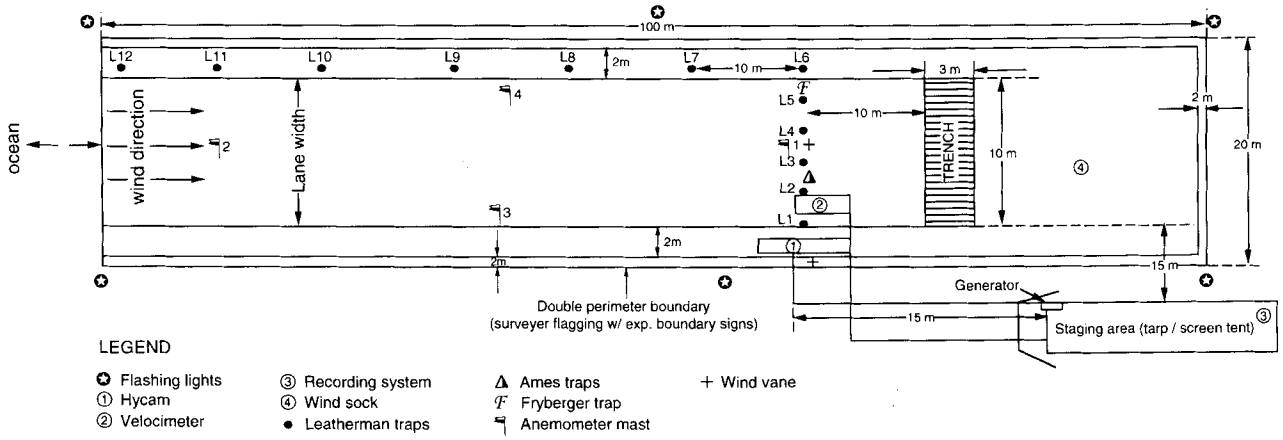

Fig. 1. Diagram of the experiment plot at Pismo Beach, California, showing the locations of apparatus and instruments. Prevailing winds come from the ocean, to the west of the plot.

and in at least one field experiment (Greeley *et al.*, 1983). These studies led to derivations of expressions relating the amount of material transported and the speeds of particles to various parameters of the wind. However, inadequate field measurements, artefacts introduced in wind tunnels or due to the design of some collectors, and assumptions made in analytical models result in uncertainties in the values reported for fluxes and particle speeds for application to the study of aeolian processes.

The goal of this investigation was to measure flux, particle speed and key parameters of the wind in a natural environment and to minimize experimentally induced artefacts. The field site was a relatively flat, homogeneous sand beach subjected to reliable, consistent onshore winds. Sand was collected in a large (surface area $=28{\cdot}8\ m^2$) trench, 50 cm deep, during a timed interval. Collection was made concurrently with measurements of wind velocities and direction, atmospheric temperatures, and particle speeds, together with acquisition of high-speed motion pictures of grains in saltation. In addition, particles were collected using various mechanical sand traps for comparison with fluxes derived from material collected in the trench. Figure 1 shows the layout of the experiment site.

The field experiment was conducted at the south end of Pismo Beach State Park, California, 6–19 May 1992 (Table 1). During this time of the year, winds are predominantly from the west-northwest and are frequently above threshold wind speeds for sand. The part of the beach selected for the study was relatively little used by the public and was undisturbed during the experiments. The beach forms a flat surface (Fig. 2) that has a fetch of about 265 m from the high tide berm along the shore to the upwind margin of the experiment plot. After the collection trench was excavated (Fig. 3) and instruments were deployed, the perimeter of the plot was marked with surveyor's flagging to restrict casual visitors (there were none) and the surface was raked smooth. The plot was further conditioned to a natural, rippled surface by sand-moving winds on 7 May prior to field measurements. For runs 5 and 6, an array of overturned buckets was placed upwind from the trench to create an artificially rough surface (Fig. 2). Each bucket was 25 cm in diameter by 25 cm high, spaced 1·5 m apart, in a staggered pattern.

Each run consisted of collecting sand in the trench during relatively constant winds for periods as long as 1·5 h. The trench was covered before and after each run. Concurrently with collection, wind speeds were recorded, the sand traps and velocimeter were activated, and high-speed motion pictures were taken. In some cases, more than one measurement was taken during a run (e.g. particle velocimeter measurements) and were assigned 'subrun' designations. Runs 1 and 2 were trial runs to test the various systems; although flux information from the trench was inadequate for analysis, valid particle velocity data were obtained from runs 1 and 2.

WIND DATA

Wind velocity profiles were obtained from four micrometeorology masts in the plot. Each mast was 9·6 m high and had an array of six cup anemometers placed at heights logarithmically

Table 1. Experiment data for runs at Pismo Beach.

	Date	Time Start	Time End	Duration (s)	Flux (g cm^{-1} s)	u_* (m s^{-1})*	z_0 (m)*	Azimuth (°)	σ
Trench run									
1	08 May 92	1330	1503	5580	†	0·489	0·022	289	5
2	13 May 92	1556	1702	3960	‡	0·312	0·0010	291	2
3	15 May 92	1412	1505	3180	0·161	0·348	0·0009	291	1
4	16 May 92	1514	1601	2820	0·0270	0·317	0·0031	283	3
5	18 May 92	1316	1401	2700	0·190	0·48	0·0032	295	2
6	19 May 92	1257	1342	2700	0·104	0·45	0·0055	290	4
Hycam run§									
1a	08 May 92	1441		6		0·47	0·01		
1b	08 May 92	1607		6		0·51	0·02		
2a	13 May 92	1605		4·1		0·31	0·0007		
3a	15 May 92	1430		4·1		0·29	0·0002		
3b	15 May 92	1452		4·1		0·35	0·0005		
4a	16 May 92	1525		4·1		0·31	0·003		
4b	16 May 92	1558		4·1		0·26	0·004		
5a	18 May 92	1332		4·1		0·54	0·003		
5b	18 May 92	1358		4·1		0·49	0·002		
6a	19 May 92	1308		4·1		0·41	0·003		
6b	19 May 92	1333		4·1		0·42	0·002		

*Averages from the four masts. †Failure of trench collector. ‡Variable wind speeds. §Run 1 at 3000 frames per second for 6 s, other runs at 5000 frames per second for 4·1 s. σ, one standard deviation of azimuth in degrees.

Fig. 2. Panoramic view of the plot, showing an array of overturned buckets used to create an aerodynamically rough surface in runs 5 and 6. Mast 1 is to the right, mast 2 is to the left (upwind), and masts 3 and 4 are on the margins of the tract. Each mast had six anemometers; mast 1 also had a wind vane and temperature sensors. The collection trench is out of view to the right. (ASU photograph 3764-A-11,12).

spaced, i.e. at 0·75, 1·25, 2·07, 3·44, 5·72 and 9·50 m (Fig. 3). Data were recorded on a Campbell Scientific CR10 system. Wind directions were recorded at two locations. Temperature measurements were made on mast 1 at heights of 1·25, 5·72 and 9·5 m in order to determine atmospheric stability.

During all six runs the wind direction was consistent from the west-northwest with little deviation in direction during the runs (Table 1). Wind speed data were reduced following the procedure given in Greeley *et al.* (in press). Wind velocity profiles generated by this method are shown in Fig. 4 for each of the six

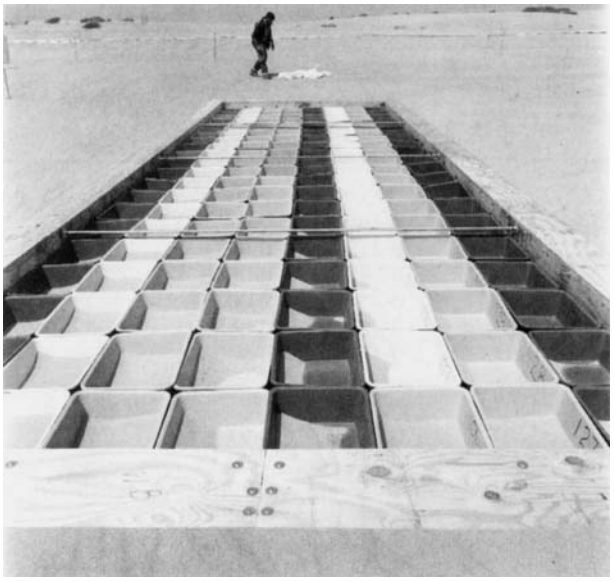

Fig. 3. View of the trench (3 m by 10 m) and the sand collection bins. Three horizontal pipes supported plywood walls to stabilize the trench. A plywood perimeter enabled access to the trench without disturbing the sand close to the trench. Prevailing winds were from left to right in this view. (ASU photograph 3763-A-23).

runs. Anemometer mast 1 was located 10 m upwind from the trench, mast 2 was located at the upwind end of the experiment plot, and masts 3 and four were on the margins of the tract (Fig. 1). Figure 4 shows that the aerodynamic roughness parameter, z_0 (average height of zero velocity), is highest at mast 2 and generally decreases toward the trench. This result is attributed to the boundary-layer response to changes in surface roughness as the wind blew across the beach from the sea and encountered a berm ~50 cm high near the high tide line. Surface roughness then decreased across the 265-m 'fetch' from the berm to the experiment plot. Sand ripples ~8 cm high occurred at the upwind end, and decreased to ~3 cm high at mast 1. During the experiment period, the heights of the ripples changed in response to wind speed, and these figures are averages, although the largest ripples were always found at the upwind end of the site. Wind data and z_0 values in Table 1 are averages from all four masts.

The artificial roughness induced by the bucket array is reflected by higher z_0 values for run 6, shown in Table 1 and Fig. 4. Although run 5 also involved the bucket array, the aerodynamic roughness, z_0, was only marginally higher than run 4. This is attributed to the wind history during 18–19 May and the response of the sand surface to the wind. Although winds increased during this interval, during run 5 the surface around the buckets was little affected. However, by the time of run 6, local scouring of sand around the buckets had generated a much rougher surface, as reflected by the high z_0 value. If this explanation is correct, then the surface roughness 'seen' by the atmospheric boundary layer was influenced more by the sand bedforms and scour features around the buckets than by the buckets alone.

SALTATION SAND FLUX

Mass flux of wind-blown sand has long been of interest in predicting sediment transport, and many workers have addressed the issue. Accurate data for transport rates are difficult to obtain, and many expressions have been derived to fit experimental data from field and wind tunnel studies. Pye & Tsoar (1990) review the problem and discuss some of the sand traps used previously in the field to measure saltation flux horizontally and vertically above the surface. Rasmussen & Mikkelsen (1994) review various systems that have been used in wind tunnels and in the field. These workers all note the difficulty in designing traps that are efficient in representing the actual quantity of blown sand, and point out that the presence of collectors in the airstream interferes with the saltation cloud and generally results in under-collection of material. Although isokinetic collectors mitigate the problem (Rasmussen & Mikkelsen, 1994), accurate flux measurements remain difficult to obtain.

Flux expressions

Table 2 lists various formulae for flux and indicates the bases for their derivation. Several of the equations account for the fact that mass transport rate should be zero at threshold (r_t=1). The value of u_{*t} in these equations should probably be the impact threshold, which is lower than the static threshold value. As reviewed by Sarre (1987), Cooke *et al.* (1993) and others, most equations relating flux to wind speed derive from Bagnold's investigations. Bagnold (1941) derived the expression for momentum loss of the air due to sand in saltation as

$$q(u_2-u_1)/L_p \sim q\ u_2/L_p=\tau=\rho\ u_*^2 \quad (1)$$

in which q is the mass of sand per unit lateral dimension per unit time, u_1 is the initial

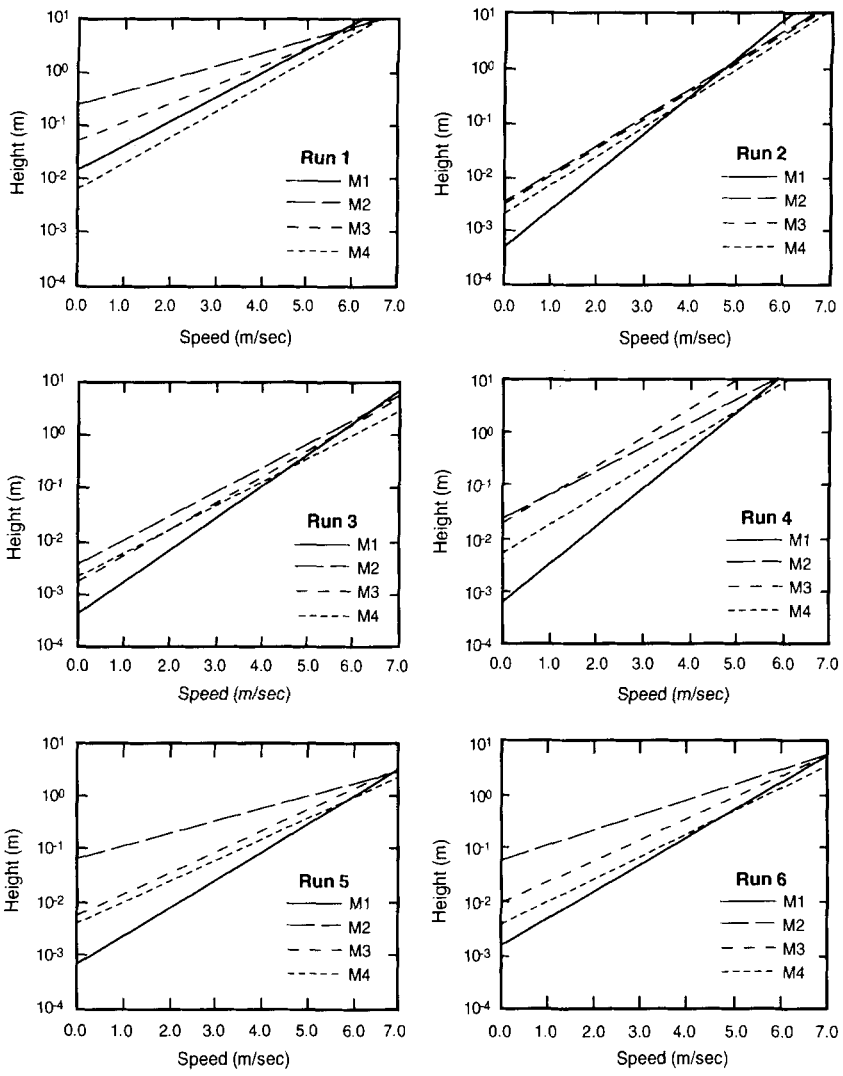

Fig. 4. Reduced wind records for the six primary runs, showing the average wind speeds vs. log height for each of the four masts (M1 to M4); the height intercept of each profile defines the aerodynamic roughness parameter, z_0.

horizontal speed (assumed small), u_2 is the final horizontal particle speed on impact, L_p is the distance travelled per grain, ρ is the fluid density and τ is the surface stress. As discussed by Greeley & Iversen (1985), this quantity represents the momentum loss per unit time per unit length of travel per unit lateral dimension, i.e. momentum loss per unit area per unit time, which is equal to force per unit area or surface stress, τ. Bagnold assumed that $u_2/L_p \sim g/w_0$, in which w_0 is the initial vertical velocity and is of the order of friction speed u_*, and g is the acceleration due to gravity; thus,

$$q \propto \rho\, u_*^2\, w_0/g \propto \rho u_*^3/g. \quad (2)$$

Based on wind tunnel experiments, Bagnold found that he could fit his data for different particle diameters (D_p) by

$$q\, g/\rho\, u_*^3 = C\,(D_p/D_{p0})^{1/2} \quad (3)$$

in which C is a function of particle size distribution and D_{p0} is 250 μm. He indicates that the

Table 2. Mass transport rate expressions.

Source	Expression
Bagnold (1941)*	$qg/\rho u_*^3 = C(D_p/D_{p0})^{1/2}$
Hsu (1973)‡	$q = k(u_*/gD^{1/2})^3$
Kawamura (1951)†	$qg/\rho u_*^3 = C(1+r_t^2)(1-r_t)$
Lettau & Lettau (1978)†	$qg/\rho u_*^3 = C(1-r_t)$
White (1979)	$qg/\rho u_*^3 = 2{\cdot}61\ (1-u_{*t}/u_*)(1+u_{*t}/u_*)$
Williams (1964)§	$qg/\rho u_*^3 = a'b'$
Zingg (1953)*	$qg/\rho u_*^3 = C(D_p/D_{p0})^{3/4}$

*D_{p0}=250 μm; C_1=1·5; C_2=1·8; C_3=2·8.
†$r_t = u_{*t}/u_*$.
‡ln k=−0·47+4·97D.
§a'=1·188; b'=3·422.

transport rate is greater (as much as twice) for a bed of particles of mixed sizes than for particles of uniform size. In addition, the latter expression (Eq. 3) is probably a function of several parameters, including the ratios of friction speed to threshold speed, and terminal speed to threshold friction speed and surface roughness.

In order to determine sand flux and to compare the results with various expressions for flux, a sand collection trench was dug across the experiment plot transverse to the wind. The collection trench was 9·6 m wide (transverse to the wind), 3 m long (parallel to the wind) and 0·5 m deep. This is more than 10 times the horizontal collection area of previous field traps, such as that of Belly (1964). The trench was lined with plywood, and numbered plastic bins 35 by 45·5 by 14·6 cm deep were placed on the floor of the trench, forming an 'egg-box' pattern to collect the sand (Fig. 2). We assumed that nearly all sand in saltation would fall into the trench and the bins, although it is possible that some saltation trajectories might exceed the 3-m length of the trench. However, some grains may have hit the edges of the bins or the support pipes and bounced out of the trench. The total surface area of these edges is less than 5% of the area of the trench. In addition, open spaces of 11 cm^2 occur at the corners where the bins join; in all, 1848 cm^2 of such voids occur, which is less than 1% of the total surface area of the trench. The flux measurements were adjusted by this percentage to allow for grains falling into the trench, but not collecting in the bins.

The entire trench was covered except during active experiment runs. During each run, the trench was uncovered for a timed interval and then re-covered when winds noticeably changed speed. Sands were then collected from each bin, bagged by bin number, weighed in the field and then stored for later analysis. For the first experiment (run 1), the cover system was faulty, and the sand surface was disturbed by footprints. Run 1 was thus used to test the system and allow the surface to recover. For the second experiment, winds were highly variable (often below threshold). Consequently, sand masses collected from the trench for runs 1 and 2 were not used in the analyses of saltation flux.

Figure 5 shows the basic relationship of flux as a function of the cube of the wind shear, developed by Bagnold (1941). Note that the increased surface roughness in run 6 (Table 1) resulted in a decrease in flux in comparison to the smoother surfaces of runs 3–5, despite the relatively higher u_*value for run 6. Figure 6 compares the flux

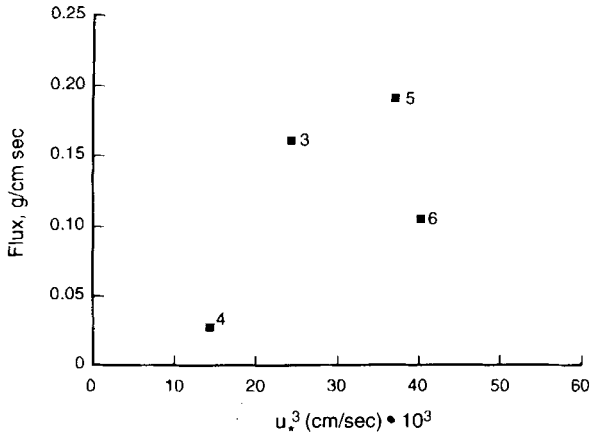

Fig. 5. Diagram showing flux as a function of u_*^3 for runs 3–6. Note the decrease in flux in run 6, which has the highest aerodynamic roughness (z_0=0·0055 m).

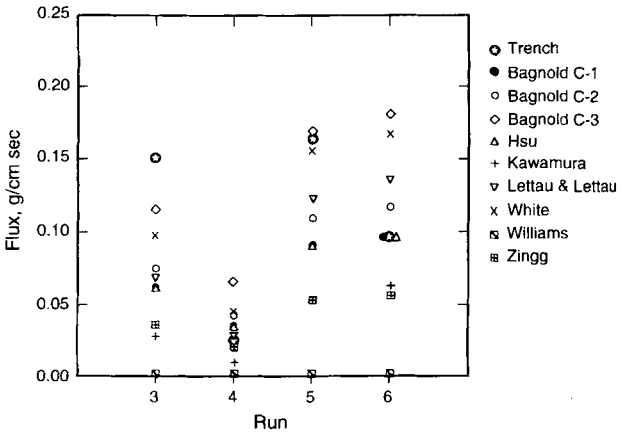

Fig. 6. Flux estimates based on various published predictions (Table 2), compared to flux determined from the trench (star symbol). Friction velocities (u_*) from mast 1 were used in the calculations. Most expressions under-predict collection of sand in comparison to the trench, except for the run 6, which was aerodynamically rough.

derived from the trench in runs 3–6 with predictions from various workers. Results show best agreement for runs 3–5 with the expression by White (1979) and Bagnold's 'C3' expression (Table 2), in which C3 is a coefficient related to particle size sorting. As noted by Blumberg & Greeley (1993), the White (1979) expression contains an error and the comparison is based on the corrected equation

$$q = 2{\cdot}61 u_*^2 \rho (1 - u_{*t}/u_*)(1 + u_{*t}/u_*)^2/g. \quad (4)$$

The best agreement (within 4·3%) is between the corrected White equation (Eq. 4) and run 5. The best agreement for run 6 (rough surface) is with Bagnold's 'C1' and Hsu's (1973) expressions.

Except for run 4 and the rough surface of run 6, most expressions tend to under-predict flux, at least in comparison to the trench. We attribute this to the derivation of most expressions being based on various sand collectors, or traps, which, as shown in the next section, are generally inefficient in representing the total flux.

Particle collectors

Most wind tunnel and field studies of flux have involved placing sand traps or various collecting devices on sandy surfaces and obtaining concurrent wind measurements. Unfortunately, many of the wind tunnels used in these studies introduce artefacts to the flow field or are too short to allow development of a saltation cloud simulating natural conditions. Moreover, many of the field studies did not adequately characterize the wind profile, nor derive surface roughness measurements, such that the friction velocity was poorly characterized.

Our goal was to compare fluxes derived from traps similar to those used in some previous studies with values obtained from sand collected in the trench. Three types of sand traps were used in the Pismo Beach experiments. The Leatherman trap (Leatherman, 1976; Rosen, 1979) consists of a plastic pipe 10·8 cm in diameter by 100 cm long with an open slit positioned toward the direction of wind flow (Fig. 7). About half the length of the pipe is buried in the sand. The traps have an effective collection area 7 cm wide by 48 cm high. Five traps of this design were deployed transverse to the wind 10 m upwind from the trench. An additional seven traps were deployed along the length of the plot, spaced 10 m apart parallel with the wind and placed *en echelon* to minimize potential interference of one trap with the next. Figure 8 shows the fluxes for the seven traps aligned with the wind for runs 2–6. In general, flux was fairly constant from the upwind area, through the plot, to the trench. The exception is run 2, during which the winds were highly variable. Local gusts probably caused collection to be sporadic among the traps. Runs 5 and 6 have the highest flux, reflecting the highest u_*values (Table 1). Because these traps were arrayed on the edge of the experiment plot parallel with the wind (Fig. 1), they were not influenced by the artificial roughness introduced with the buckets.

The Fryberger trap (Fryberger *et al.*, 1984), modified from a design by Bagnold (1938), consists of a wind vane connected to a collection blade, the front of which is open and provides a collecting area 1 cm wide by 120 cm high (Fig. 9). It is designed to rotate so that the collection area always faces into the wind. The third sand trap (Ames trap) consists of wedge-shaped semi-isokinetic collectors that were designed for use at the NASA–Ames wind tunnels (Greeley *et al.*, 1982). Each collector has a 1-cm^2 collection area and can be stacked, thus enabling flux as a function of height above the surface to be measured. One stack 45 cm high was placed in the experiment plot (Fig. 1).

Fig. 7. Typical Leatherman trap (Leatherman, 1976) used in the Pismo Beach experiments. Traps were covered with a cloth case except during active collection intervals, which were timed. (ASU photograph 3763-A-13).

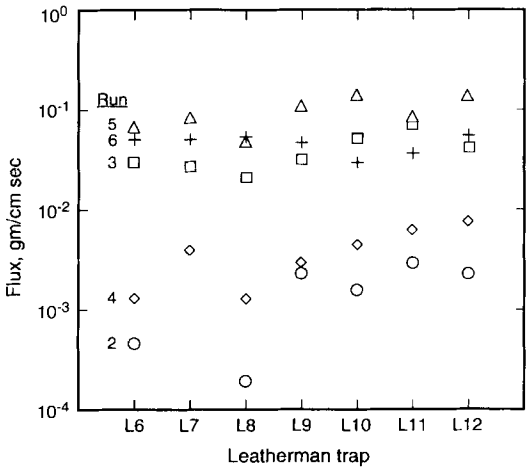

Fig. 8. Flux derived from the Leatherman traps arrayed parallel to the wind; L-6 was closest to the trench, L-12 was at the upwind end of the experiment plot; numbers by the symbols indicate the run.

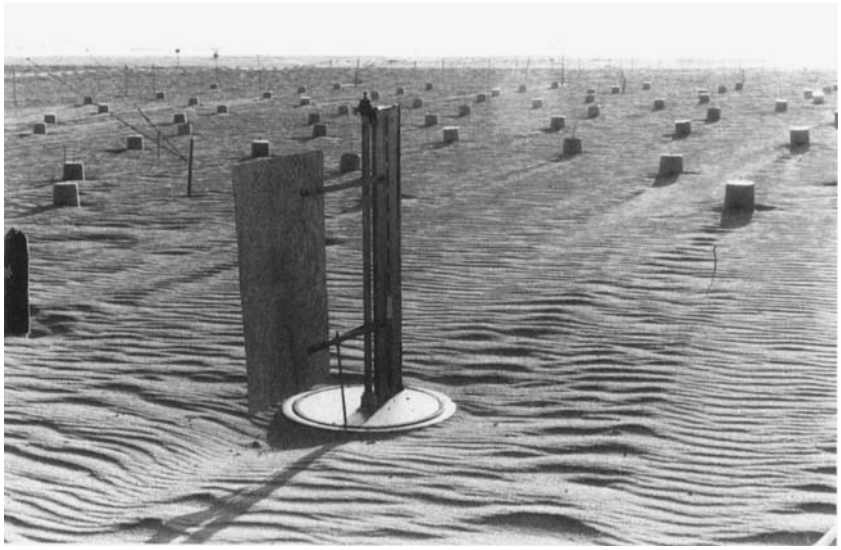

Fig. 9. Fryberger trap (modified Bagnold design) in place during run 6. Note the influence of the buckets on the surface roughness, with sand scour around each bucket and the formation of large ripples in the wake of the buckets. (ASU photograph 3766-D-32).

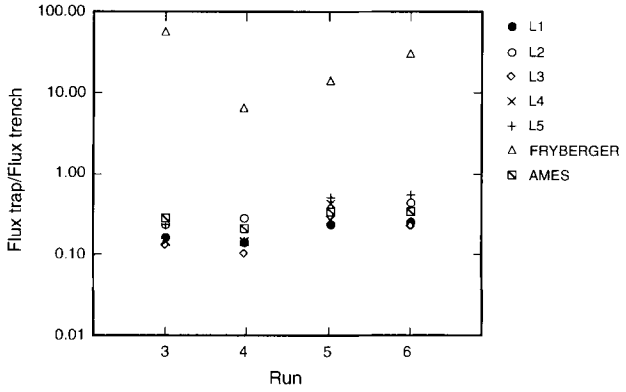

Fig. 10. Comparison of normalized fluxes derived from various sand traps compared to the flux derived from the trench. A value of 1 would indicate perfect correlation. The high values for the Fryberger trap are attributed to sand leaking into the base of the collector before and after the timed interval of the runs.

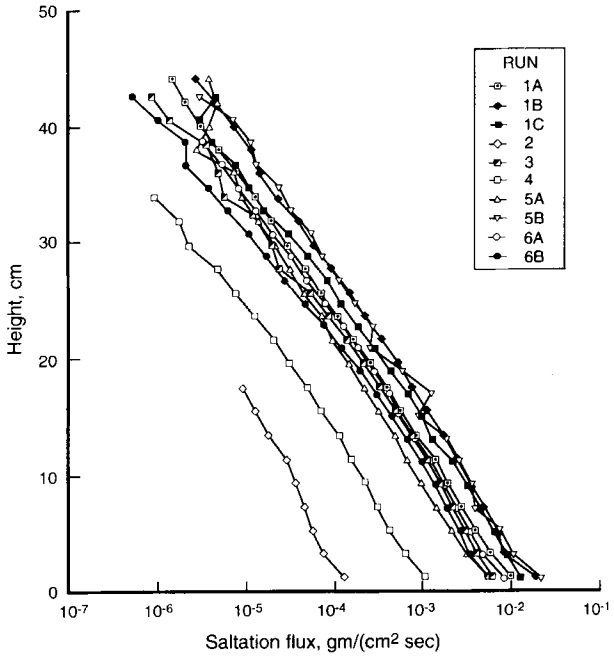

Fig. 11. Flux as a function of height derived from the Ames sand traps.

Figure 10 compares fluxes derived from the various sand collectors to the flux derived from the trench. In this plot, a perfect correlation would have a value of 1. The Ames trap and the five Leatherman traps in front of the trench are consistent with each other, but all tend to undercollect material by about 70% in comparison to the trench. This is probably due to the interference to both the airflow and saltation cloud created by the presence of the collector, as noted by previous workers (Rasmussen & Mikkelsen, 1994). The Fryberger trap consistently overcollected material in comparison to the trench. This is attributed to leakage of sand into the collector through the swivel joint between the wind vane and the base at times when there should have been no sand collected.

Figure 11 shows the flux of particles in 1-cm increments of height derived from the Ames collector stack for 10 runs. There is a clear log-linear decrease in sand flux with height. Note also the decrease in flux with wind speed (Table 1).

PARTICLE SPEEDS

Speeds of particles in the saltation cloud were measured using a velocimeter and were also derived from analyses of high-speed motion

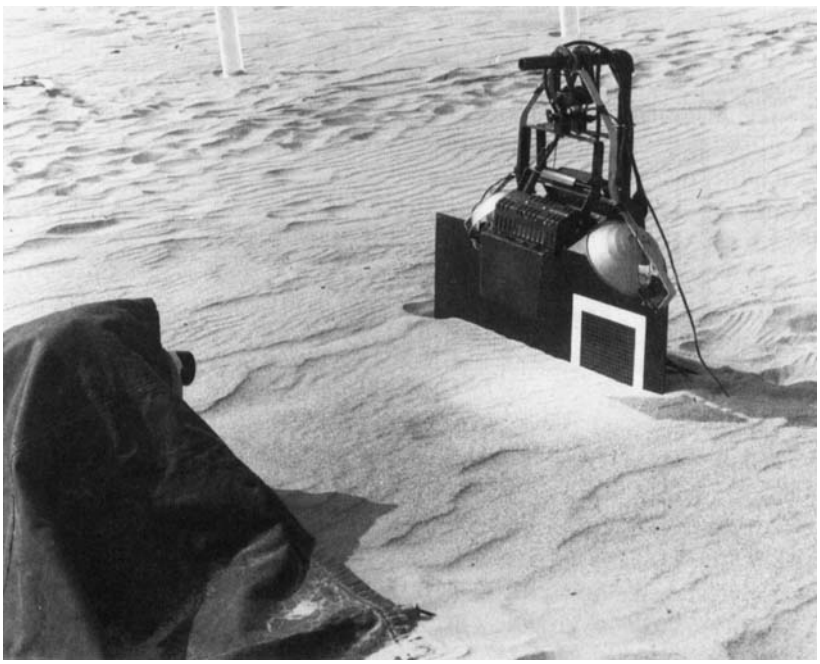

Fig. 12. Set-up for obtaining high-speed motion pictures (3000 and 5000 frames per second) of saltating sand grains; camera (covered with cloth) is on the left; grains saltated from left to right in front of a black back-drop; flashbulbs were used to illuminate the scene during an active run. (ASU photograph 3762-A-4).

pictures. High-speed motion pictures were obtained for grains in saltation at the edge of the experiment plot (Fig. 1) using a Redlake Hycam camera (Fig. 12) set at a filming rate of 3000 (run 1) and 5000 (runs 2–6) frames per second. The field of view was about 3 by 3 cm, centred at a height of 2 cm above the surface. A 'backdrop' was provided by a black plate with a white grid pattern in 1-cm cells. Filming against this plate enabled individual grains to be resolved in-flight. Although the plate and supporting structure for lights obstructed the wind, placement minimized interference with the trajectories of the saltating grains that were filmed. Eleven film sequences were obtained during the field study (Table 1).

The films were analysed by projecting images onto a digitizing tablet. Individual grains were tracked along their trajectories and it was noted whether they were on ascending or descending paths. From the framing rate and the scale on the backdrop, velocities of the grains were determined. Figure 13 shows combined results for runs 3a and b, for which 93 particles were analysed. The histograms show that most particles have speeds centred around 1·5–2 m s^{-1}. Descending particles have slightly higher speeds in comparison to ascending particles, as would be expected because descending grains are exposed to the wind for a longer time.

Particle speeds were also measured using a velocimeter based on a design by Schmidt (1977). This instrument produces a light beam perpendicular to the wind stream, focused on two phototransistors that detect the shadow of particles as they cross two separate parts of the light beam. Parallel windows limit the field of view of the light receivers; an electronic unit connects the two phototransistors such that a

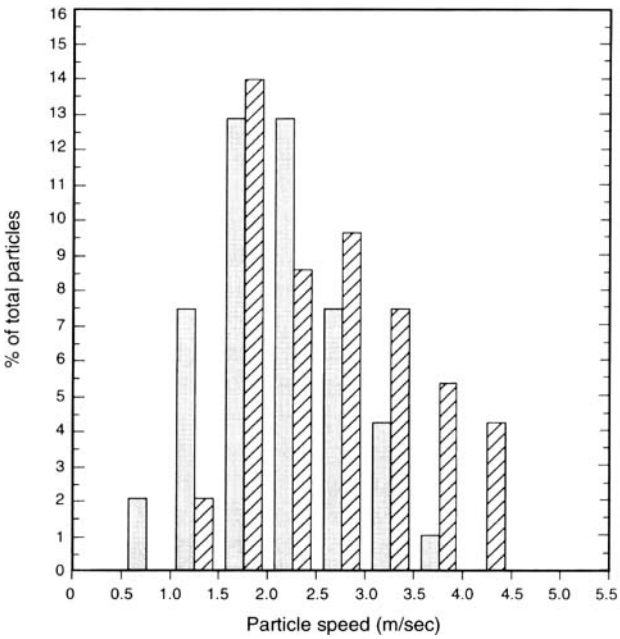

Fig. 13. Histogram showing distribution of particle speeds derived from analysis of high-speed motion pictures of runs 3a and b; shaded bars represent grains on ascending part of saltation trajectory; cross-hatched bars are for descending part of trajectory.

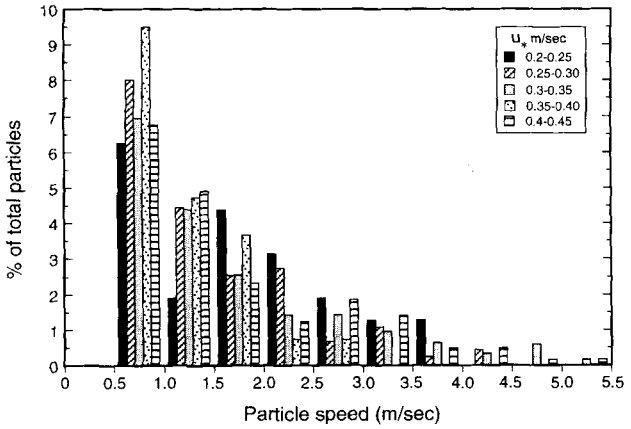

Fig. 14. *Particle speed distributions measured by the velocimeter at a height of 2 cm above, given for five ranges of wind friction velocities from run 5.*

particle passing through the light beam produces a positive voltage pulse as it shadows the first window, and a negative pulse at the second window. To determine particle speed, the time interval between positive and negative pulses is measured with an oscilloscope. This time interval, in conjunction with the known separation of the sensor windows, enables the particle velocity to be determined.

The velocimeter was placed in the plot (Fig. 1) to measure the speeds of grains at a height of 2·0 cm above the surface. Over the six runs, particle speeds ranged from 0·5 to 7·0 m s^{-1}. Figure 14 shows particle velocimeter data taken during run 5. The speeds of 738 particles were analysed and correlated with concurrent wind measurements, expressed in u_*, which ranged from 0·2–0·45 m s^{-1}. Most particles (~59%) had speeds less than 1·5 m s^{-1}. Less than 3% of the grains exceeded speeds of 4 m s^{-1}. Based on analysis of the Hycam pictures, the higher speed grains are probably on the descending part of the saltation trajectory.

The particle velocimeter data showed a particle speed distribution similar to the Hycam results at higher speeds. At low speeds, however, the velocimeter apparently detected many more slow-moving particles than were seen in the film, resulting in a particle distribution that monotonically declines from the slowest measurable particle speed. This could be attributed to the design of the velocimeter. If a grain enters the slot at an angle and triggers the 'start' transistor only, the timer will run for a very brief time without a 'stop' signal before resetting. If another grain triggers the 'stop' transistor while the timer is running, a false speed value is indicated. Because the probability of such an event increases with count time, as does the false value of the speed, there will be many more false slow-speed readings than high-speed ones.

PARTICLE SIZE ANALYSIS

Sand samples were obtained for each of the 168 bins for each run. The goal was to study the grain size distribution across the trench to determine trends that could be attributed to mode of transport, and to evaluate the homogeneity of the saltation cloud transverse to the wind. Pismo Beach sands have a modal distribution of ~230 μm. A coarser fraction (~1200 μm) occurs as a lag deposit on large ripples.

Preliminary analysis of particle sizes from the bins shows several trends (Hartmann *et al.*, 1994). Figure 15 shows modes for grains along three traverses across the trench parallel to the wind, one traverse on the north side, one down the middle and one on the south side of the trench. Data are included for runs 2, 3, 4 and 6. In general, the first bins on the upwind side of the trench have the largest grains. This is attributed to material moving in creep or reptation that is immediately trapped as it encounters the trench. The last two or three bins closest to the downwind side of the trench also show an increase in modal size. Although a clear explanation is lacking, these slightly larger grains may have had more elastic rebound in saltation, resulting in longer trajectories to reach the far side of the trench. Run 6 involved the rougher (bucket array) surface. In this run, the modal sizes for most bins are lower than for the other runs. This is attributed to the reduction of wind energy by the rougher surfaces and the attendant decrease in the transport of larger particles.

SUMMARY AND CONCLUSIONS

A field experiment was conducted at Pismo Beach, California, to obtain data on sand flux and particle speeds in a natural environment. A trench 3 by 10 m positioned transverse to the wind enabled collection of virtually all wind-blown sand during timed intervals. Concurrent wind velocity and temperature profiles were obtained during each run so that wind friction velocities and aerodynamic roughness heights could be derived. Various sand traps (Leatherman, Ames and Fryberger systems) were

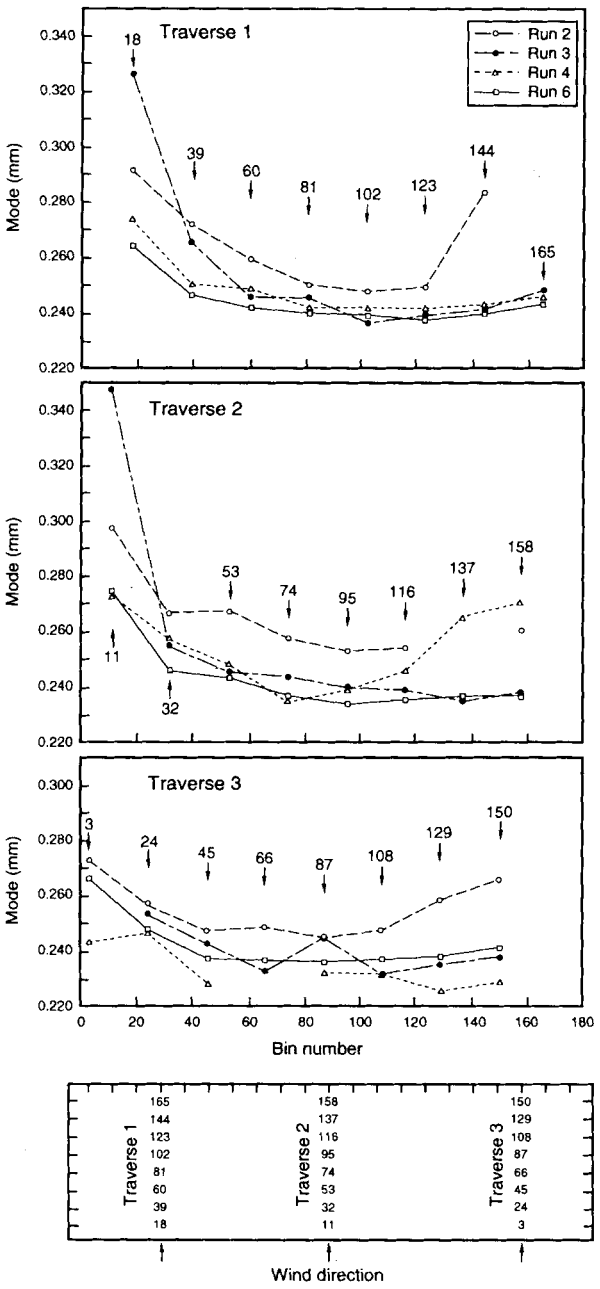

Fig. 15. Modal grain sizes along three traverses across the trench parallel with the wind; lower figure shows the trench, wind direction and position of the three traverses; numbers correspond to the collection bins. Note that the modal grain size is largest in the bins on the upwind end of each traverse, reflecting collection of material in creep.

also deployed. Use of a particle velocimeter and high-speed motion pictures (3000 and 5000 frames per second) enabled particle speeds to be determined. Individual collecting bins inside the trench provide information on flux and grain size distributions as a function of location.

Preliminary analysis includes the following results.

1 The Leatherman and Ames particle collectors yielded fluxes about 70% less than the values determined from the trench, in confirmation of previous observations that most collectors interfere with the air flow and saltation cloud, inhibiting collection of grains. The Fryberger trap over-collected material, but this appears to be due to a faulty seal at the base of the swivel mechanism.

2 Most published expressions for particle flux yielded values that were also less than the flux measured in the field from the trench. This could be because most expressions are derived from wind tunnel experiments and field studies in which inefficient particle collectors were used. The expressions of Bagnold (1941) and White (1979) were within 35 and 4·3% of our field values for runs 3 and 5, respectively. Sarre (1987) also finds that White's (1979) expression is closest to fluxes Sarre measured in the field. However, he used the incorrect White expression. Moreover, the Sarre field fluxes were based on Leatherman traps, which under-collect.

3 Analysis of particle speeds shows that grains in the descending part of their saltation trajectory have a slightly higher speed than ascending grains.

4 Particle size distributions in the trench show: (a) larger modal size in the upwind side of the trench–this probably reflects grains in creep; (b) slightly larger modal size toward the downwind side of the trench–this may reflect grains with higher elastic rebound resulting in larger trajectories.

ACKNOWLEDGMENTS

We are grateful for the assistance provided by Dan Ball, Gary Beardmore and Devorah Blumberg during the field experiments. We also thank Dan Ball and Sue Selkirk for producing the figures and Byrnece Erwin for word processing. Finally, we acknowledge with gratitude the help of Don Patton, District Superintendent, and the Rangers of the Pismo Dunes State Vehicular Restricted Area and Dan Blankenship, Resource Ecologist. This study was supported by the Office of Planetary Geosciences, National Aeronautics and Space Administration. We thank M. A. Rice and K. Stigler for their comments which helped improve the manuscript.

REFERENCES

Anderson, R.S. and Hallet, B. (1986) Sediment transport by wind: toward a general model. *Bull. geol. Soc. Am.*, **97,** 523–535.

Bagnold, R.A. (1938) The measurement of sand storms. *Proc. Roy. Soc. London, Ser. A,* **167,** 282–291.

Bagnold, R.A. (1941) *The Physics of Blown Sand and Desert Dunes.* Methuen, London.

Belly, P.Y. (1964) Sand movement by the wind. *U.S. Army Corps of Engineers, Coastal Eng. Res. Ctr. Tech. Memo no. 1.*

Blumberg, D.G. and Greeley, R. (1993) Field studies of aerodynamic roughness length. *J. Arid Environment,* **25,** 39–48.

Cooke, R., Warren, A. and Goudie, A. (1993) *Desert Geomorphology.* UCL Press, London.

Fryberger, S.G., Al-Sari, A.M., Clisham, T.J., Rizvi, A.R. and Al-Hinai, K.G. (1984) Wind sedimentation in the Jafurah Sand Sea, Saudi Arabia. *Sedimentology,* **37,** 23–43.

Greeley, R., Blumberg, D.G., Dobrovolskis, A.R., Gaddis, L.R., Iversen, J.D., Lancaster, N., Rasmussen, K.R., Saunders, R.S., Wall, S.D. and White, B.R. (in press) Potential transport of windblown sand: Influence of surface roughness and assessment with radar data. In: *Desert Aeolian Processes* (Ed. by V. P. Tchakerian), Chapman & Hall, New York.

Greeley, R. and Iversen, J.D. (1985) *Wind as a Geologic Process.* Cambridge University Press, Cambridge.

Greeley, R., Leach, R.N., Williams, S.H. White, B.R., Pollack, J.B., Krinsley, D.H. and Marshall, J.R. (1982) Rate of wind abrasion on Mars. *J. geophys. Res.,* **87,** 10,009–10,024.

Greeley, R., Williams, S.H. and Marshall, J.R. (1983) Velocities of windblown particles in saltation: preliminary laboratory and field measurements. In: *Eolian Sediments* and *Processes* (Ed. by M. E. Brookfield and T. S. Ahlbrandt), pp. 133–148. Elsevier, Amsterdam.

Hartmann, D., Blumberg, D.G. and Greeley, R. (1994) The Pismo Beach experiment: Grain size characteristics and patterns. In: *Response of Eolian Processes to Global Change,* Desert Research Institute, Quaternary Sciences Center, *Occasional Paper 2,* pp. 49–50.

Hsu, S.A. (1973) Computing eolian sand transport from shear velocity measurements. *J. Geol.,* **81,** 739–43.

Kawamura, R. (1951) Study on sand movement by wind. *Institute of Science and Technology, Tokyo, Report,* **5,** 95–112.

Leatherman, S.P. (1976) Barrier island dynamics: over wash processes and eolian transport. *Proc. 15th Confr. Coastal Engng.,* pp. 1958–1974.

Leatherman, S.P. (1978) Short communication: a new aeolian sand trap design. *Sedimentology,* **25,** 303–306.

Lettau, K. and Lettau, H.H. (1978) Experimental and micro-meteorological field studies of dune migration. In: *Exploring the World's Driest Climate* (Ed. by H. H. Lettau and K. Lettau), *University of Wisconsin-Madison, Inst. for Environ. Studies, IES Report,* **101,** 110–147.

Owens, J.S. (1927) The movement of sand by wind. *Engineer,* **143,** 377.

Pye, K. and Tsoar, H. (1990) *Aeolian Sand and Sand Dunes.* Unwin Hyman Ltd, London.

Rasmussen, K.R. and Mikkelsen, H.E. (1991) Wind tunnel observations of aeolian transport rates. *Acta Mechanica (Suppl.),* **1,** 135–144.

Rasmussen, K.R. and Mikkelsen, H.E. (1994) The aeolian transport rate profile and the efficiency of sand traps (in press).

Rosen, P.S. (1978) An efficient, low cost, aeolian sampling system. *Sci. Tech. Notes, Current Res., Part A Geol. Surv. Canada Paper,* **78–1A,** 531–532.

Sarre, R.D. (1987) Aeolian sand transport. *Prog. Phys. Geog.,* **11,** 157–182.

Schmidt, R.A. (1977) A system that measures blowing snow. *Res. Paper RM-19.*S. Department of Agriculture, Washington, DC.

Sorensen, M. (1991) An analytic model of wind-blown sand transport. *Acta Mech. (Suppl.),* **1,** 67–81.

White, B.R. (1979) Soil transport by winds on Mars. *J. geophys. Res.,* **84,** 4643–51.

White, B.R. and Schulz, J.C. (1977) Magnus effect on saltation. *J. Fluid Mechanics,* **81,** 497–512.

Willetts, B.B. and Rice, M.A. (1986) Collision in aeolian transport: the saltation/creep link. In: *Aeolian Geomorphology* (Ed. by W. G. Nickling), pp. 1–17. Allen & Unwin, Inc., Winchester.

Williams, G. (1964) Some aspects of the eolian saltation load. *Sedimentology,* **3,** 257–287.

Zingg, A.W. (1953) Wind tunnel studies of the movement of sedimentary material. *Proc. 5th Hydraulic Conf. Bull.,* **34,** 111–35.

Manuscript received 3 November 1994; revision accepted 6 June 1995.